Low-energy behavior of exothermic dissociative electron attachment

Ilya I. Fabrikant
Department of Physics and Astronomy, University of Nebraska, Lincoln, Nebraska 68588-0111

Hartmut Hotop
Fachbereich Physik, Universität Kaiserslautern, D-67653 Kaiserslautern, Germany

(Received 30 June 2000; published 10 January 2001)

We discuss two models for electron attachment to molecules: the Vogt-Wannier model for capture into a polarization well and the resonance model for dissociative attachment. The Vogt-Wannier model is generalized for the case of a target with a permanent dipole moment, and results are presented for dissociative attachment to CH_3I. It is shown that the resonance theory should incorporate in this case a weakly bound dipole-supported state of CH_3I^-, whereas the generalized Vogt-Wannier theory gives a reasonable estimate for the cross section in the meV and sub-meV region. The Vogt-Wannier model is also applied to the process of attachment to SF_6, CCl_4, and C_{60}. In the first case the s-wave capture model provides a satisfactory description of the experimental data for energies below the first vibrational excitation threshold, whereas for CCl_4 it underestimates the attachment cross section by a factor of 2 in the sub-meV region. For C_{60} we suggest that electron attachment is dominated by *s*-wave capture in the region below 2 meV and by *p*-wave capture in the energy range above 4 meV. Our model reproduces data for Rydberg electron and free-electron attachment observed in beam experiments. It is, however, at variance with the strong rise of the attachment rate coefficients with electron temperature observed in flowing afterglow–Langmuir probe measurements.

DOI: 10.1103/PhysRevA.63.022706 PACS number(s): 34.80.Ht

I. INTRODUCTION

Dissociative attachment cross sections are very sensitive to the details of the electron-molecule interaction and the coupling between the electron scattering channels and the dissociating channels. Exothermic dissociative attachment (DA) reactions might exhibit very large cross sections at low energies; however, this region is not well studied theoretically. Even qualitative aspects of the low-energy behavior of the exothermic DA reaction are not yet well understood. According to the Bethe-Wigner law [1], for nonpolar molecules the cross section should depend on energy E as $E^{l-1/2}$, where l is the lowest angular momentum allowed by the symmetry of the intermediate negative-ion state. However, the coefficient of proportionality in this law appears to be very different in different theoretical approaches. According to the theory of O'Malley [2] and of Bardsley [3] in the local approximation the cross section is given by (atomic units are used throughout the paper)

$$\sigma = \frac{\pi^2}{E}\Gamma |F_C|^2 s \tag{1}$$

where Γ is the width of the intermediate negative-ion state in the Franck-Condon region, $|F_C|^2$ is the Franck-Condon factor for the transition between the initial state and the negative-ion state, and s is the survival factor. At low energies the energy dependencies of the Franck-Condon factor and of the survival factor are relatively weak, and the threshold behavior is given by the energy dependence of Γ/E $(\sim E^{l-1/2})$.

A completely different approach is used in applying the Vogt-Wannier (VW) model for the capture into a polarization well [4]. It is assumed there that the reaction occurs with 100% probability if the electron falls into the singularity created by the polarization potential $-\alpha/2r^4$. The cross section depends only on energy and the molecular polarizability α, and in the low-energy region it is given by the simple formula

$$\sigma = 4\pi(\alpha/2E)^{1/2}. \tag{2}$$

The original VW result, Eq. (37) of Ref. [4], was derived from the theory of Mathieu functions. However, for the *s*-wave contribution Klots [5] was able to find a simple expression

$$\sigma = \frac{\pi}{2E}[1-\exp\{-4(2\alpha E)^{1/2}\}] \tag{3}$$

which fits very well the exact Vogt-Wannier result for $l=0$ and describes the transition from the low-energy behavior (2) to the unitarity limit $\pi/2E$ at higher energies.

The Vogt-Wannier (VW) model seems to be unphysical in the sense that the actual long-range potential does not have a $1/r^4$ singularity. So far a detailed comparison with the VW limit has only been possible for the molecules SF_6 and CCl_4 which are among the few molecules that do not have a permanent dipole or quadrupole moment and thereby lend themselves to a comparison with the VW model. Both Rydberg electron transfer (RET) and laser photoelectron detachment (LPA) experiments have yielded experimental results down to sufficiently low energies to make a meaningful comparison with the VW model possible. Klar *et al.* [6,7] have used a variant of the Klots formula (3) to describe their LPA cross sections, measured at sub-meV resolution, by a simple analytical formula,

$$\sigma = \frac{\sigma_0}{E}[1-\exp(-\beta\sqrt{E})]. \tag{4}$$

The product $\sigma_0\beta$ corresponds to the VW coefficient $4\pi(\alpha/2)^{1/2}$ with two adjustable parameters, σ_0 and β.

Although both Eqs. (1) and (2) [or (4)] give the same energy dependence for *s*-wave electrons, there is no relation between them otherwise. The VW model does not incorporate the resonance mechanism; therefore there is no resonance characteristic like a width in their equation.

The situation turns out to be even more complicated for dipolar molecules. If the electron energy is large compared to the rotational spacing (an assumption that holds down to sub-meV energies for relatively heavy molecules), the Bethe-Wigner threshold law should be modified [8]. For subcritical dipole moments, $\mu<\mu_{\rm cr}=0.6395$ a.u., the cross section becomes proportional to $E^{\lambda-1/2}$ where λ is a threshold exponent whose value varies between 0 for $\mu=0$ and $-1/2$ for $\mu=\mu_{\rm cr}$. The local approximation, Eq. (1), is consistent with this modification. However, the VW theory has never been extended to polar molecules. In addition, the low-energy behavior for scattering by polar targets can be strongly affected by very diffuse dipole-supported bound or virtual states [9,10]. It is known that these states lead to enhancement of the cross sections. However, there is no theory predicting how big this enhancement is for the DA process.

The present paper studies low-energy dissociative attachment for several targets. First we extend the VW treatment to polar targets, and then we calculate the DA cross section for the methyl iodide molecule using three different methods: extended Vogt-Wannier (EVW), the local version of the O'Malley-Bardsley theory, and the nonlocal resonance theory. Then we analyze the low-energy behavior of DA for several nonpolar targets. We show that the VW or the EVW approach might be appropriate at very low electron energies (below the first vibrational excitation threshold), where nonadiabatic capture into a weakly bound state becomes possible. The local version of the resonance theory is unable to describe this effect, although the complete treatment of vibrational dynamics which incorporates weakly bound states (for example, the resonance *R*-matrix theory) can describe both resonant and nonresonant attachment.

II. EXTENDED VOGT AND WANNIER THEORY

The VW theory assumes the absorption boundary condition at the origin due to capture into the polarization well. The reaction cross section σ_r in this case is given by [11]

$$\sigma_r = \frac{\pi}{k^2}\sum_{ll'}(\delta_{ll'}-|S_{ll'}|^2), \tag{5}$$

where $S_{ll'}$ are the matrix elements of the scattering operator in the angular momentum representation.

The Schrödinger equation for a superposition of the dipolar and polarization potentials allows separation of the variables. The wave function can be expanded in dipolar angular harmonics [12,13] and the radial equation has the form

$$\left(\frac{d^2}{dr^2}+k^2-\frac{\lambda(\lambda+1)}{r^2}+\frac{\alpha}{r^4}\right)u(r)=0, \tag{6}$$

where $k^2=2E$ and $\lambda(\lambda+1)$ is an eigenvalue of the operator $L^2-2\mu\cos\theta$, where L^2 is the square of the orbital angular momentum. For subcritical dipole moments considered here $\lambda(\lambda+1)>-1/4$ and λ is real.

The scattering matrix can also be transformed into the dipolar angular harmonics representation where it becomes diagonal. In the low-energy region only the lowest eigenvalue λ makes a contribution to the inelastic cross section, which can now be written in the form

$$\sigma_r = \frac{\pi}{k^2}(1-|S_0|^2), \tag{7}$$

where S_0 is the matrix element of the scattering operator corresponding to the lowest λ.

The required solution of the radial equation with the ingoing-wave boundary conditions at the origin has the following asymptotic form at $r\to 0$:

$$u(r)\sim \text{const}\times re^{i\zeta}, \quad \zeta=\alpha^{1/2}/r-\pi\lambda/2. \tag{8}$$

The radial wave function u can be written in terms of real functions f and g

$$u=g+if \tag{9}$$

with the boundary conditions

$$f\sim r\sin\zeta, \quad g\sim r\cos\zeta. \tag{10}$$

At large r, $u(r)$ can be written as

$$u(r)=\phi^{(-)}-S_0\phi^{(+)}, \tag{11}$$

where

$$\phi^{(\pm)}\sim\exp[\pm i(kr-\lambda\pi/2)] \tag{12}$$

at $r\to\infty$.

For determination of S_0 we need to find the connection between two pairs of solutions: f,g and $\phi^{(\pm)}$. As in the Vogt and Wannier paper, this is possible by using the Mathieu functions. However, in this paper we will consider the low-energy region where the energy dependence of S_0 can be expressed through elementary functions. For this purpose we introduce a new pair of real solutions $v^{(\pm)}$ which are connected with $\phi^{(\pm)}$ by the equation

$$\phi^{(\pm)}=v^{(-)}-\frac{e^{\mp i\pi\tau}}{\sin\pi\tau}v^{(+)}, \tag{13}$$

where $\tau=\lambda+1/2$. At large r, $v^{(\pm)}$ behave as

$$v^{(+)}\sim\sin(kr-\pi\lambda/2), \tag{14}$$

$$v^{(-)}\sim\cos(kr-\pi\lambda/2)+\tan\pi\lambda\sin(kr-\pi\lambda/2). \tag{15}$$

The explicit representation for $v^{(\pm)}$ at $k\to 0$ was given in Ref. [13]:

$$v^{(\pm)}=A^{\pm}\frac{\Gamma(\mp\tau+1)}{\Gamma(\pm\tau+1)}\left(\frac{\pi kr}{4}\right)^{1/2}\left(\frac{k\alpha^{1/2}}{4}\right)^{\pm\tau}J_{\mp\tau}\left(\frac{\alpha^{1/2}}{r}\right), \tag{16}$$

where Γ is the gamma function, J is the Bessel function, and $A^{+}=1$, $A^{-}=1/\cos(\pi\lambda)$.

Using the asymptotic expression for the Bessel functions at large arguments, we immediately obtain the required connection formulas

$$v^{(+)}=b(g\cos\pi\lambda-f\sin\pi\lambda), \quad v^{(-)}=\frac{f}{b\cos\pi\lambda}, \tag{17}$$

where

$$b=\frac{\Gamma(1-\tau)}{2^{2\tau}\Gamma(1+\tau)}(k\alpha^{1/2})^{\tau}. \tag{18}$$

We have assumed the same arbitrary constant in the definition of f and g. Its specific value does not affect S_0.

We express now f and g in terms of $v^{(\pm)}$, use the relation between $v^{(\pm)}$ and $\phi^{(\pm)}$, and compare the result with Eq. (11). Finally we have

$$S_0=\frac{1/b-b}{1/b+b\exp(-2\pi i\lambda)} \tag{19}$$

and

$$1-|S_0|^2=\frac{4\cos^2\pi\lambda}{b^2+1/b^2+2\cos 2\pi\lambda}. \tag{20}$$

Note that, although b is asymptotically small, the threshold exponent τ might be close to 0, as, for example, in the case of CH_3I; therefore Eqs. (19) and (20) should not be simplified further. In particular, using $1-|S_0|^2=4b^2\cos^2\pi\lambda$ for the CH_3I molecule violates the unitarity limit even at the electron energy $E=0.01$ meV.

Note that, for zero dipole moment μ, $\lambda=0$, $\tau=1/2$, and $b^2=k\alpha^{1/2}$ which gives the correct VW limit, Eq. (2). On the other hand, when μ approaches the critical value $\mu_{\rm cr}=0.6395$ a.u. we have $\lambda\to -1/2$, and Eqs. (19) and (20) exhibit an uncertainty of the type 0/0, which should be resolved by using l'Hôpital's rule. Since this case is of no practical importance, we do not elaborate on it further.

III. RESONANCE THEORY

For comparison of the EVW theory with the resonance theory we use the resonance R-matrix approach [14,15] in which the fixed-nuclei R matrix as a function of internuclear distance ρ is given by one diagonal matrix element

$$R(\rho)=\frac{\gamma^2(\rho)}{W(\rho)-E}+R_b, \tag{21}$$

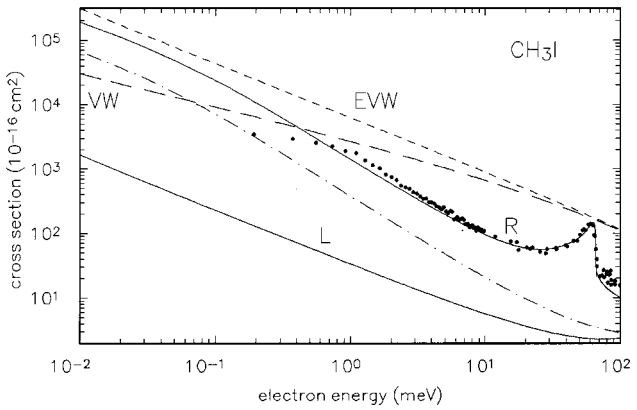

FIG. 1. Low-energy dissociative electron attachment to methyl iodide. Solid curves: *R*, complete *R*-matrix calculations; L, local approximation. Dot-dashed curve: two-channel approximation. Long-dashed curve (VW): VW model. Short-dashed curve: EVW model. Full circles: laser photoelectron attachment measurements obtained for a supersonic beam target [15].

where $W(\rho)$ is the lowest R-matrix pole and R_b is a background term weakly dependent on ρ.

The S-matrix elements for DA can be written in the matrix form

$$S_{\rm DA}=2\pi i(\tilde{u}^{+})^{-1}(1+\gamma G^{(+)}\gamma L^{+})^{-1}y, \tag{22}$$

where $\tilde{u}^{+}=u^{+}-R_b(u^{+})'$, u^{+} and $(u^{+})'$ are the diagonal matrices of the electron radial wave functions and their derivatives corresponding to outgoing-wave boundary conditions in different vibrational channels ν, $L^{+}=(u^{+})'/\tilde{u}^{+}$, $G^{(+)}$ is the Green's function for the nuclear motion in the negative-ion state, and y is the vector of the first-order amplitudes

$$y_{\nu}=\langle\nu|\gamma|\psi^{(+)}\rangle, \tag{23}$$

where $\psi^{(+)}$ is the nuclear wave function describing the motion in the negative-ion state.

In what follows we will also consider a simplified version of the resonance theory whereby we neglect the operator $\gamma G^{(+)}\gamma$ in the resonance denominator of Eq. (22). Using a known connection [14] between the R-matrix theory and the Feshbach approach, we can show that the cross section in this approximation is given by O'Malley's Eq. (1), or the local approximation, with $s=1$. Since at low electron energies the survival probability is close to 1, we will refer to this approximation as the local approximation.

IV. LOW-ENERGY ATTACHMENT TO CH_3I

A. Comparison of EVW with *R*-matrix results: role of dipole-supported states

In Fig. 1 we present the DA cross section for methyl iodide molecules in the vibrational ground state CH_3I ($\nu_3=0$) calculated using different theories: the Klots fit of the

VW result, the EVW (including the dipole moment) result, the complete *R*-matrix calculations, and the results of the local approximation.

First of all we see very large deviations between the different theories, reaching two orders of magnitude for a fixed energy, with the lowest cross sections obtained with the local theory and the highest with the EVW theory. The energy dependence of the cross section at ultralow energies is determined by the threshold exponent $\tau=\lambda+1/2$. For CH_3I $\tau=0.034$ is close to zero, therefore both the extended Vogt and Wannier model and the local theory predict a fast growth of the cross section approaching $E^{-0.965}$. However, the nonlocal results above 0.1 meV exhibit an even faster variation. In addition, the nonlocal cross sections are much greater (typically almost two orders of magnitude) than those of the local calculations, in agreement with recent experimental data [15] shown in the figure. The *R*-matrix cross section near the threshold for vibrational excitation of the symmetric C-I stretch is dominated by a vibrational Feshbach resonance which was discussed in detail in Ref. [15]. All other calculations do not exhibit this resonance. We note that this vibrational Feshbach resonance occurs only in DA to CH_3I ($\nu_3=0$).

In order to understand the physical significance of these results, we will discuss first the equation describing the threshold behavior of the cross section for a process involving electrons interacting with a polar molecule with $\mu<\mu_{cr}$. According to the general theory [8,16] in the case of an exothermic reaction we have

$$\sigma=\frac{ck^{2\lambda-1}}{|\eta-ie^{-i\pi\lambda}k^{2\lambda+1}|^2}, \tag{24}$$

where η is a complex parameter. If only one (elastic) channel is open, η is real, and the scattering *S* matrix has a pole in the complex energy plane which corresponds to a bound state at $\eta<0$ and a virtual state at $\eta>0$. (Note, however, that this is not a conventional virtual state, since the pole is not lying on the imaginary axis in this case [17].) In the former case the binding energy is given by

$$-k^2=(-\eta)^{1/\tau}. \tag{25}$$

The calculated cross section in the energy range between 0.01 and 1 meV can be fitted by Eq. (24) with $\eta=-0.661$ which corresponds to a bound state with the energy 0.07 meV. However, this is not a true bound state: since the DA channel is open even for negative electron energies, the bound state CH_3I^- can decay into CH_3 and I^-. Therefore the *S*-matrix pole has a nonzero imaginary part and both η and k^2 in Eq. (25) are complex. Our calculations of the dynamical *S* matrix at negative electron energies show that the real part of the pole is close to –0.07 meV; therefore $\mathrm{Im}\,\eta=0$ is a good approximation for the description of the DA cross sections below 1 meV. This result can be connected with the existence of the vibrational Feshbach resonance below the $\nu_3=1$ threshold whose width is substantially larger because of the lower potential barrier for the nuclear motion for the $\nu_3=1$ state. The resonance disappears at $\nu_3=2$ [15].

We conclude that the big value of the DA cross section for methyl iodide in the ultralow-energy region can be explained by the influence of the dipole-supported state which is not incorporated into the local version of the resonance theory. To confirm this, we have completed one more set of calculations, which can be called the two-channel approximation, and corresponds to inclusion of only one channel in the resonance denominator of Eq. (22). In this manner we incorporate two channels for the nuclear motion, the initial vibrational state of the neutral and the final dissociative channel, and ignore vibrationally excited states. This approximation incorporates approximately the dipole-supported state near the $\nu_3=0$ threshold. The results are substantially higher than the local calculations but still lie below the ''exact'' *R*-matrix results. The two-channel approximation also does not describe the structure below the $\nu_3=1$ threshold.

B. Rotational effects

The above discussion did not take into account rotation. Methyl iodide is a prolate symmetric top whose rotational spectrum is given by [18]

$$E(J,K)=BJ(J+1)+(A-B)K^2, \tag{26}$$

where J and K are rotational quantum numbers for a symmetric top. For a prolate symmetric top the states with $K>0$ are rarely populated at room temperature; therefore for the discussion of rotational effects the first term in Eq. (26) is the most important. The rotational constant B for methyl iodide equals 0.037 meV; therefore the cross section behavior below 0.1 meV should be calculated with the inclusion of rotational motion. Rotation restores the Wigner law. A similar effect can be caused by Λ doubling. This was demonstrated in photodetachment experiments [19] where the transition from the dipole threshold law to the Wigner law was observed. Rotation has been shown to destroy the dipole-supported state for methyl chloride [20], and we can expect similar effects for other molecules, even in their ground rotational states. Moreover, many rotational states are typically populated in experiments, and we should expect deviations from Eq. (24) even at higher energies.

Experimental data [15] presented in Fig. 1 indicate that the deviations from the threshold law (24) start to occur below 1 meV even for a supersonic beam target. (Note, however, that the rotational state distribution in this case is unknown.) A similar deviation is observed in measurements performed at room temperature [15], which is consistent with an estimate for the rotational splitting $\Delta E\sim(Bk_BT/2)^{1/2}$ at room temperature. The slope of the experimental curve below 1 meV becomes consistent with the original Vogt-Wannier result, demonstrating transition from the dipole threshold law to the Bethe-Wigner law. However, experimental data for a supersonic target were obtained at higher current level and broader energy width and are not as accurate at low energies as room-temperature data. On the other hand, the room-temperature results contain contributions of higher vibrational states and cannot be directly compared

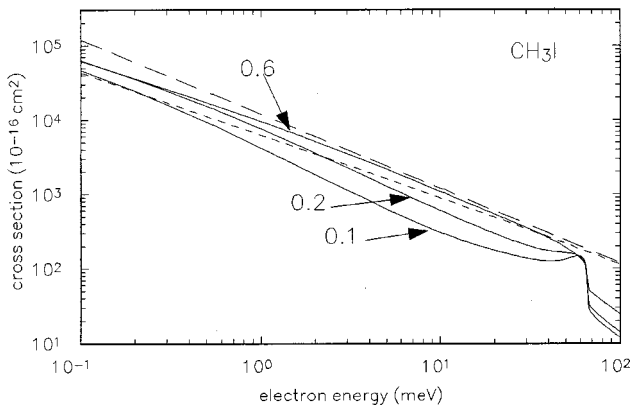

FIG. 2. Dissociative attachment to methyl iodide. Solid curves were obtained by using different solvation energies: 0.1, 0.2, and 0.6 eV. Short-dashed curve: EVW model. Long-dashed curve: the unitarity limit π/k^2.

with the theory presented in Fig. 1. (Comparison of theory with the room-temperature results is presented in Ref. [15].)

Note that the Bethe-Wigner law $E^{-1/2}$ can be substantially modified due to the dipole-supported states even in the μeV region [9,10], and therefore more experimental studies in the sub-meV region are desirable.

C. Solvation effect

According to Fig. 1, the EVW model gives very large cross sections that are close to the unitarity limit π/k^2 at energies above 1 meV. Physically this means that the combination of the dipolar and polarization potentials acts as a ''black'' sphere making the reaction cross section close to the elastic cross section. One might think that the extended Vogt-Wannier model provides an upper bound for the cross section. However, by changing the parameters of the resonance theory, it is possible to obtain even higher cross sections.

To demonstrate this, we present in Fig. 2 the results of *R*-matrix calculations with negative-ion curves that were shifted down by different amounts. Physically these calculations approximately describe the solvation effects in attachment to clusters [21]. The cross sections for the different solvation energies stay close to the EVW results, but might even exceed them. As the solvation energy increases, the width of the vibrational Feshbach resonance (VFR) grows. At ultralow energies this effect lowers the slope of the cross section as a function of energy, although it remains somewhat higher than the slope of the EVW curve. Near the $\nu_3=1$ threshold the effect leads to the disappearance of the VFR [21].

The original VW theory, without accounting for the dipolar interaction, gives cross sections that are too low in the low-energy region.

V. ELECTRON ATTACHMENT TO MOLECULES WITHOUT PERMANENT DIPOLE OR QUADRUPOLE MOMENT

A. Electron attachment to SF_6 and CCl_4

Both SF_6 and CCl_4 are among the few molecules for which the Vogt-Wannier capture model should be applicable in view of missing electric dipole and quadrupole moments, and it is of interest to compare the prediction of the VW theory with experimental results for the energy-dependent attachment cross section, obtained at very low energies and high resolution.

Using energy-variable photoelectrons from vacuum ultraviolet photoionization of rare gas atoms (energy range 0–160 meV), Chutjian and Alajajian [22] obtained clear evidence for *s*-wave behavior of the attachment cross section at low energies. Subsequently, Klar *et al.* [6,7,23,24] used a laser photoelectron attachment method with a similar energy range, but substantially improved energy width (below 1 meV). As an important ingredient and improvement over previous work, they analyzed the effects of residual electric fields (reduced to values below 1 V/m) on the near-threshold attachment yield through model calculations of the attachment yield [6,24–26]. They used the analytical cross section (4) which was found to provide a very good description of the experimental attachment yield from threshold up to the first vibrationally inelastic onset for both SF_6 [6,25,26] and CCl_4 [7,24]. In this way they were able to determine the parameter β in Eq. (4) to within 10% and thereby quantify the deviations of the cross section from the limiting behavior $\sigma(E\rightarrow 0)$ which—in terms of Eq. (4)—is given by $\sigma(E\rightarrow 0)=\sigma_0\beta/E^{1/2}$. With β expressed in units of $(\mathrm{meV})^{-1/2}$ Klar *et al.* obtained $\beta=0.405(40)$ for SF_6 [6] and $\beta=0.59(6)$ for CCl_4 [7,24], in both cases distinctly larger than the prediction obtained from the Klots formula (3), namely, $\beta_K=0.228$ for SF_6 and $\beta_K=0.299$ for CCl_4.

By normalizing their relative attachment yields to reliable thermal attachment rate coefficients $k_e(T=300\ \mathrm{K})$ [27,28], Klar *et al.* determined the constant σ_0 in Eq. (4) and thus the quantity $\sigma_0\beta$ which is a direct measure of the limiting rate coefficient $k_e(E\rightarrow 0)$ [6,24–26]. For SF_6, Schramm *et al.* [23] recently measured the attachment yield at residual electric fields of about 0.01 V/m and negligible laser bandwidth for electron energies from 10 meV down to 20 μeV; they confirmed the results of Klar *et al.* [6] for the parameter β. For CCl_4, the experimental energy resolution was not as high as for SF_6; at residual electric fields of about 0.5 V/m, the effective energy width was (slightly below) 1 meV [24]. Correspondingly, the extrapolation to the VW limit is somewhat less certain than for SF_6, but model calculations including the residual fields and the cross section (4) yielded very good agreement between the modeled and the measured attachment yield for CCl_4 in the threshold region [24]. The values for β, σ_0, and $k_e(E\rightarrow 0)$, determined experimentally for SF_6 (formation of long-lived SF_6^-) and CCl_4 (Cl^- formation), are summarized in Table I. For comparison we have listed the VW result for the capture rate coefficient k_c,

$$k_c=4\pi(\alpha/m)^{1/2}=7.755\times 10^{-8}\alpha^{1/2}\ \mathrm{cm^3\,s^{-1}}\ \ (\alpha\ \text{in atomic units}), \tag{27}$$

as well as rate coefficients k_{nl} for Rydberg electron transfer from Refs. [9,30,31] at high principal quantum numbers, at which k_{nl} was found to be independent of n for both SF_6 and

TABLE I. Molecular properties and electron attachment characteristics for SF_6 and CCl_4 at gas temperatures of $T_G = 300$ K.

Property	SF_6	CCl_4
α (units of a_0^3)	44.1 [a]	75.6 [a]
μ (D)	0	0
k_c (10^{-7} cm^3 s^{-1})	5.15 [b]	6.74 [b]
k_e ($T=300$ K) (10^{-7} cm^3 s^{-1}) (electron swarms)	2.27(9) [c]	3.79(19) [d]
k_{nl} (10^{-7} cm^3 s^{-1}) (RET)	4(1) [e]	11(2) [f]
$\sigma_0(10^{-20}$ m^2 meV)	7130(360) [g]	11160(560) [h]
β_K [(meV)$^{-1/2}$] [i]	0.228 [i]	0.299 [i]
β [(meV)$^{-1/2}$]	0.405(40) [g]	0.59(6) [h]
$k_e(E\rightarrow 0)(10^{-7}$ cm^3 s^{-1})	5.4(8) [g]	12.3(19) [h]

[a]Reference [29].
[b]Using Eq. (27) and polarizabilities in first column.
[c]Reference [27].
[d]Reference [28].
[e]Reference [30].
[f]Reference [9].
[g]Reference [6] (LPA).
[h]Reference [24] (LPA).
[i]Coefficient according to Klots formula (3).

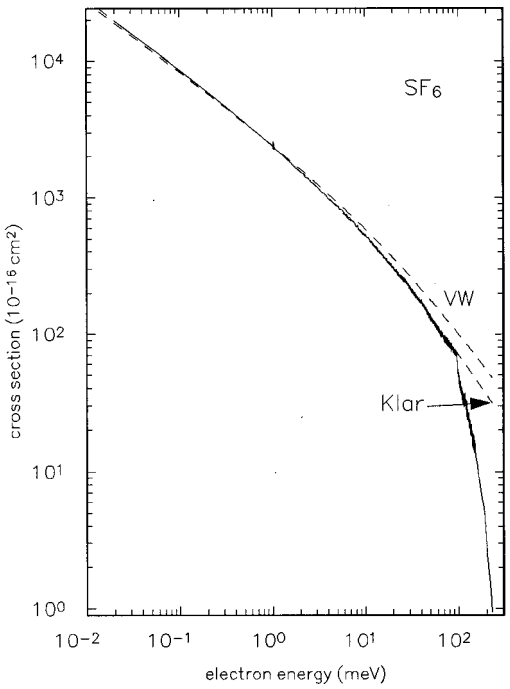

FIG. 3. Electron attachment to SF_6. Solid curve, the recommended experimental values; dashed curve VW, the prediction of the VW model; dashed curve Klar, parametrization of Klar *et al.* [6]. Note that the curve VW is indistinguishable from the Klots result, Eq. (3), on the scale of drawing.

CCl_4 (for a more detailed discussion of the RET data and their comparison with free-electron results, see [26,31]).

For SF_6, the RET value at high n $k_{nl}=4.0(10)\times10^{-7}$ cm^3 s^{-1} [30] and the LPA result for $k_e(E\rightarrow0)=5.4(8)\times10^{-7}$ cm^3 s^{-1} [6] are both in satisfactory agreement with the VW capture rate coefficient $k_c=5.15\times10^{-7}$ cm^3 s^{-1}. In Fig. 3 we present a comparison of the experimental attachment cross sections with the VW result [the latter is indistinguishable from the Klots result (3) on the scale of the drawing], and with the empirical fit of Klar *et al.* [6]. The empirical fit gives a good description of the cross section up to the threshold for ν_1 vibrational excitation where the cross section exhibits a sharp downward cusp described theoretically by Gauyacq and Herzenberg [32].

Since in the case of *s*-wave scattering there is no centrifugal barrier to support the resonance state, the process of low-energy attachment in this case can be viewed as a direct nonadiabatic capture [33,34]. Attachment to SF_6 was discussed in terms of nonadiabatic coupling by Gauyacq and Herzenberg [32]. The low-energy electron can give up its energy to become bound if the crossing of the negative-ion curve with the neutral curve occurs close to the equilibrium internuclear separation. However, there should be a mechanism preventing the electron from escaping into the continuum. In the case of SF_6 this occurs due to a fast redistribution of the available energy over many vibrational modes, before the nuclear framework can oscillate back to its initial configuration [32]. The SF_6^- anion becomes metastable, and this explains the nondissociative feature of low-energy attachment to SF_6. Since the capture in this case is nonresonant, the VW model becomes appropriate. Of course a $1/r^4$ singularity, which plays an essential role in the VW model, is unphysical. However, for sufficiently high α it describes quite well the probability of finding the electron within the molecule where direct energy exchange is likely to occur.

For CCl_4, $k_{nl}=11(2)\times10^{-7}$ cm^3 s^{-1} [9,31] and the LPA result $k_e(E\rightarrow0)=12.3(19)\times10^{-7}$ cm^3 s^{-1} [7,24] are compatible with each other, but they are both distinctly higher than the VW capture rate coefficient $k_c=6.74\times10^{-7}$ cm^3 s^{-1}. This is demonstrated in Fig. 4 by comparing the recommended experimental cross section with the VW prediction and the parametrization of Klar *et al.* [24]. The slope of the experimental curve is higher than that given by the VW model. Our discussion of methyl iodide suggests that this might be indicative of a weakly bound negative-ion state. Indeed, as was suggested by Burrow *et al.* [35], the ground $^2A_1$ CCl_4^- state is bound with a very small binding energy, whereas the first repulsive excited state $^2T_2$ has a vertical attachment energy of 0.94 eV. It is likely that the $^2T_2$ state drives the resonant DA process whereas the $^2A_1$ state enhances this process at low energies.

B. C_{60}

Low-energy electron attachment to C_{60} has been a subject of some controversy. Flowing afterglow/Langmuir probe (FALP) measurements [36,37] indicated that electron capture by C_{60} is characterized by an activation barrier of 0.26 eV. This was interpreted as a *p*-wave process by Tosatti and Manini [38] who showed that an *s* state of the C_{60}^- anion is prohibited by symmetry. Their calculations of the capture rates based on a finite potential well model are in good

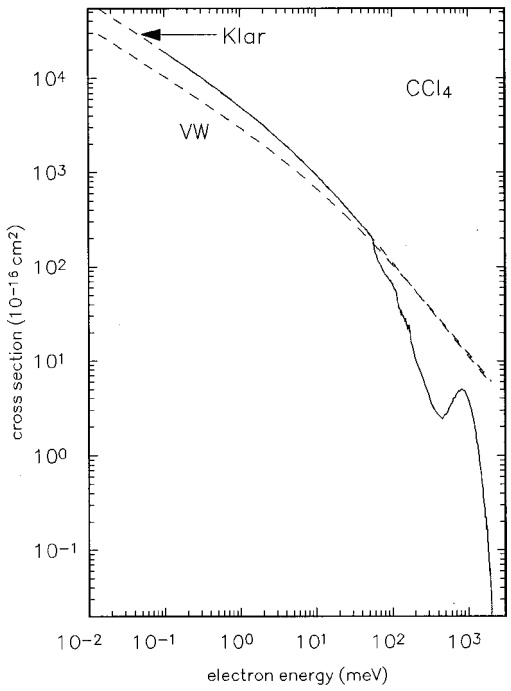

FIG. 4. Electron attachment to CCl_4. Notation is the same as in Fig. 3.

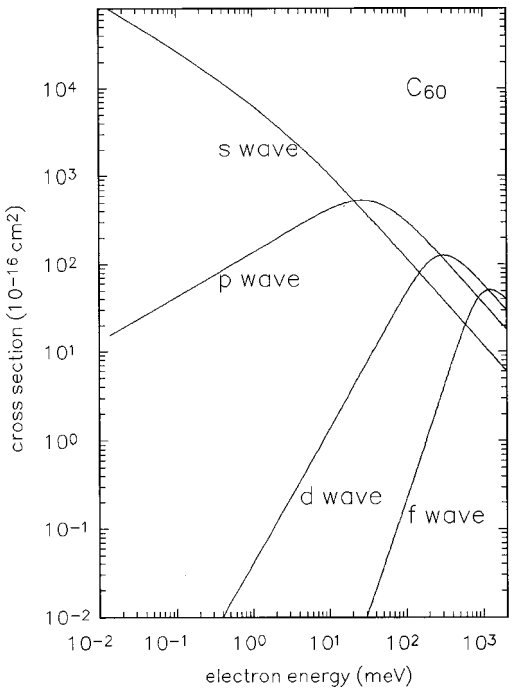

FIG. 5. Cross section for electron attachment to C_{60}: VW model for *s*-, *p*-, *d*-, and *f*-wave capture.

agreement with the FALP measurements [36,37], in terms of both the absolute magnitude and the slope of the rate dependence on the inverse electron temperature which gives the magnitude of the activation barrier.

However, as noted previously by Huang *et al.* [39], the model used in Ref. [38], and later in [40], does not seem to represent the physics of the process correctly. First, it ignores the polarizability of C_{60} which is very large (558 a.u.). Furthermore, it regards the capture cross section as being identical to the elastic cross section which is physically incorrect. The simplest way to see this is by looking at the threshold behavior: whereas the *p*-wave capture cross section behaves as $E^{1/2}$ at low energies, the elastic *p*-wave scattering cross section is proportional to E^2. The extra factor $E^{3/2}$ in the elastic cross section appears because the electron has to tunnel through the centrifugal barrier a second time when leaving the interaction zone. Therefore the good agreement between the FALP experiments and the calculations [38] seems to be fortuitous.

Several beam measurements [39–41] also claim the existence of an activation barrier with a height of 0.24 [41] or 0.15 eV [39]. However the threshold detected by Huang *et al.* [39] is likely due to experimental problems in penetrating to very low energies. The measurements of Jaffke *et al.* [41] were reinterpreted by Weber *et al.* [42] who concluded that they can only be understood if an *s*-wave contribution or a resonance close to zero energy is present. Note that the deconvoluted results in [41] were incorrectly shifted on the energy scale by 0.4 eV (see Appendix in [42]), thereby suggesting a barrier; this, however, was an artifact of the deconvolution procedure in [41].

The absence of an activation barrier is indicated by experiments on Rydberg electron attachment to C_{60} [39,42,43]. They do not confirm the *p*-wave model [38] and exhibit a flat dependence of the attachment rate on the principal quantum number of the Rydberg electron. In addition, a recent beam experiment [44] with free electrons has found evidence of a zero-energy attachment process (within 0.03 eV) which does not agree with the FALP [36,37] and the earlier beam [40,41] results. Several mechanisms for *s*-wave attachment involving formation of weakly bound [42] or virtual [45] states of C_{60}^-, supported by the long-range polarization interaction, have been discussed.

Here we will compare the obtained experimental information with the results of application of the VW model. In Fig. 5 we present the $l=0$ through $l=3$ contributions to the cross sections for capture by a target with the polarizability 558 a.u. We see that the $E^{1/2}$ behavior for the *p* wave occurs within a very narrow energy range: the *p*-wave cross section peaks at $E=26$ meV. This means that the experimental data of Elhamidi *et al.* [44] do not contradict the concept of the *p*-wave process at low energies.. On the other hand, it is obvious that this behavior does not agree with the FALP results and earlier beam experiments [40,41], which are more consistent with a *d*-type or *f*-type behavior.

Recent *ab initio* theoretical calculations [45] of elastic e-C_{60} scattering suggest that in the low-energy region this process is dominated by a virtual state in the a_g symmetry, whose lowest partial-wave component is $l=0$, and a resonance state in the t_{1u} symmetry, whose lowest partial-wave component is $l=1$. Therefore we can assume that the attachment process at low energies is controlled by a combination of direct capture mediated by a virtual state (similar to low-energy attachment to SF_6) and resonance capture into the t_{1u} state. Theoretical calculations were performed at equilibrium nuclear configuration, and nothing is known yet about the

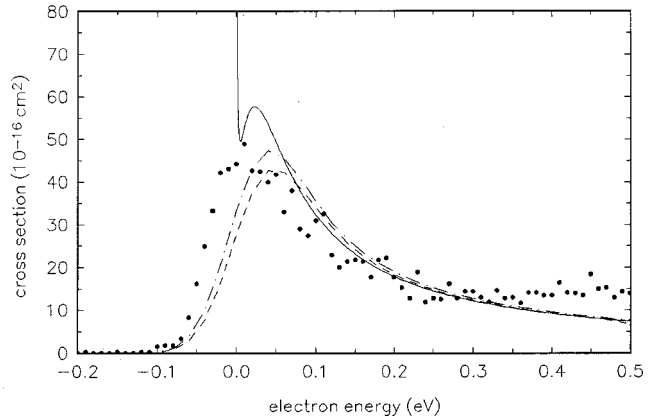

FIG. 6. Cross section for attachment to C_{60}. Solid line, calculation employing combination of *s*-wave and *p*-wave VW cross sections, Eq. (28), with $\epsilon=0.1$. Dashed line, theoretical cross section averaged over Gaussian profile with the width 50 meV. Dot-dashed line, the same average of the cross section with $\epsilon=0.2$. Circles, experimental data of Elhamidi *et al.* [44], normalized to theory at $E=0.2$ eV.

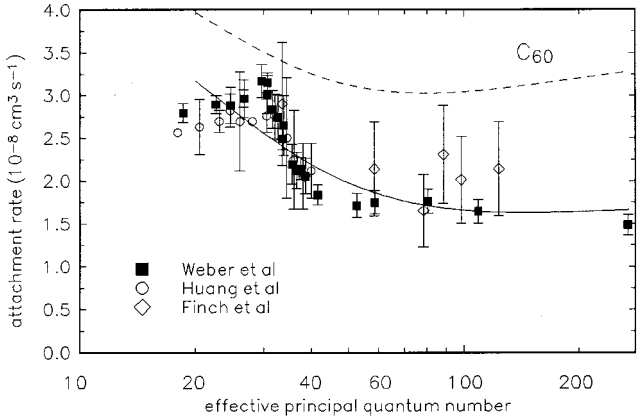

FIG. 7. Rates for Rydberg electron transfer to C_{60}. Solid curve, calculation employing Eq. (28) with $\epsilon=0.1$. Dashed curve, the same with $\epsilon=0.2$. Experimental data are those of Weber *et al.* [42] (solid squares), Huang *et al.* [39] (open circles), and Finch *et al.* [43] (open diamonds). Experimental results of Weber *et al.* were normalized to the theoretical value at $n^*=109$. All other experiments were normalized to those of Weber *et al.* at $n^*=38$.

vibrational dynamics involved. Therefore at this stage we will try to describe the capture cross section by combining the *s*-wave and the *p*-wave VW cross sections σ_0 and σ_1:

$$\sigma=c(\epsilon\sigma_0+\sigma_1), \tag{28}$$

where c and ϵ are adjustable parameters: ϵ characterizes the relative contribution of the *s* wave, and c the absolute value of the cross section which can be estimated from experimentally obtained attachment rates [39,42,43].

In Fig. 6 we present the attachment cross sections calculated with $c=\epsilon=0.1$. The s-wave zero-energy peak dominates the cross section at very low energies below 3 meV. As a result of insufficient energy resolution, the beam measurements [41,44] in the low-energy region are dominated by the *p*-wave contribution. To compare with the experiment of Elhamidi *et al.* [44] we have averaged the calculated cross sections over a Gaussian distribution with a width of 50 meV. The width was obtained from an analysis of the SF_6^- yield measured in [44]. To illustrate the influence of the *s*-wave contribution, we also present the averaged cross sections calculated with $\epsilon=0.2$. Further increase of the *s*-wave component leads to rates in the meV region which are too high compared to the experimental estimates [39,42,43].

The theoretical curve is somewhat shifted toward higher energies relative to the experimental curve, but this shift is within the experimental uncertainty of the absolute energy scale in [44]. Otherwise agreement is good, and this indicates the dominance of the resonant *p*-wave process from above about 3 meV. At higher energies other resonances found in Ref. [46] appear to drive the attachment process. We have done a similar comparison with the results of Jaffke *et al.* [41], as revised by Weber *et al.* [42], by averaging the theoretical cross section over a Gaussian distribution of width 200 meV. The position of the experimental peak is shifted toward somewhat higher energy in this case. To compare with the FALP data, we have averaged the theoretical results over Maxwellian electron energy distribution and obtained rate coefficients that are nearly independent of electron temperature, whereas the FALP experiments exhibit an increase of an order of magnitude over the range $T=300$–1500 K.

Note that only 1–2 % ($c\epsilon=0.01$ or 0.02) of the *s*-wave VW cross section appears to contribute to the capture process, in contrast with attachment to SF_6. Apparently the stabilization mechanism discussed for SF_6 is not as efficient for C_{60}. The 1–2 % fraction can be considered as an efficiency for conversion of the C_{60}^- virtual state into a bound state, something similar to the survival probability in resonance attachment.

In Fig. 7 we present the attachment rate for Rydberg electrons calculated by using the Fermi free-electron model [47] with semiclassical electron velocity distributions (see, e.g., [26]). The *s*-wave contribution dominates at $n>60$ and makes the rate as a function of n essentially flat. The overall increase of the experimental rates toward lower n is described well by the theory. However, the free-electron model does not reproduce the stepwise structure in the region $n=30$. Apparently the influence of the Rydberg core, which can mediate formation of C_{60}^- via a curve-crossing mechanism [48], becomes important in this region.

We think that the following conclusions can be drawn from the above comparisons. First, the result of the recent beam experiment [44] is consistent with a dominant *p*-wave capture process. In the meV energy range *s*-wave capture, possibly mediated by a virtual state, becomes important, and this is demonstrated experimentally by the results on Rydberg electron capture at high n. The temperature dependence of the attachment rate coefficient observed in the FALP experiments [36,37] is not in accord with the combined *s* and *p* model. Possibly, the electron energy distribution in the temperature-variable FALP apparatus is not completely thermalized and short of low-energy electrons. Another possibility is a significant dependence of the negative-ion yield on the rovibrational temperature of C_{60}. The C_{60} temperature in

the free-electron and Rydberg electron beam experiments [39–44] is between about 600 and 940 K. In the FALP experiment C_{60} was vaporized at a temperature of 700 K, but the temperature of the attaching C_{60} molecules was uncertain, ''presumably less than 700 K and probably close to the carrier gas temperature of 300 K'' [37].

VI. CONCLUSIONS

The VW and EVW models in many cases give reasonable estimates for attachment cross sections, and for the SF_6 target the VW prediction is in fact in very good agreement with experiment. One may ask whether these models reflect the physics of low-energy attachment, or whether they are just a convenient way to interpolate the cross section between the threshold behavior and the unitarity limit. Indeed, DA is typically a resonance process, and any equation for the DA cross section should contain the resonance width, like the O'Malley formula, Eq. (1). The VW formula, which is actually an equation for the capture cross section, does not contain a width. In most cases the VW-type formula works as an empirical fit, Eq. (4), in contrast to the Klots formula, Eq. (3) (basically equivalent to the original VW result), which does not contain adjustable parameters.

However, our discussion of low-energy attachment for several molecules shows that the VW and EVW models can be employed when the process is controlled by nonadiabatic capture into a weakly bound or virtual state. This mechanism certainly plays a role in attachment to SF_6, CCl_4, and CH_3I, and, very likely, in attachment to C_{60}.

Another good example is electron attachment to metal clusters [49]. In this case the nonresonance capture appears to occur in many partial waves. The summation of VW cross sections over all contributing partial waves yields a result that, at high enough energies, is close to the well-known Langevin cross section for capture of a classical particle [50]

$$\sigma_{cl}(E) = \pi(2\alpha/E)^{1/2}. \tag{29}$$

[It is interesting that the classical capture cross section equals exactly half of the low-energy limit of the VW *s*-wave cross section, Eq. (2), as emphasized by Vogt and Wannier [4]]. Equation (29) describes very well the experimental results [49] for attachment to sodium clusters. The mechanism for nonresonant nondissociative capture might be enhanced in this case due to the much larger number of degrees of freedom in clusters. However, it has not been studied yet how the excess energy is redistributed in this process.

In the case of CCl_4 we have—in addition to the CCl_4^- symmetric ground state $^2A_1$ [35], whose binding energy is close to zero at equilibrium—a resonance $^2T_2$ state [35] which increases the attachment probability. Therefore the attachment cross section exceeds the VW result in this case. The exothermic resonance path makes low-energy attachment to CCl_4 dissociative (production of Cl^-).

The situation with polar molecules is somewhat different. The case of DA to CH_3I discussed above is described very well by resonance *R*-matrix theory. However, at very low (or near-threshold) electron energy an alternative approach incorporating nonadiabatic capture into a diffuse dipole-supported bound state might be valid. In fact this state appears as a vibrational Feshbach resonance [15] near the threshold for excitation of the symmetric C-I stretch. Therefore it might be not surprising that the EVW model, in contrast to the local approximation (1), gives a reasonable order-of-magnitude estimate for the cross section in this case. Both mechanisms (resonance and nonadiabatic capture) are incorporated into the *R*-matrix formalism. In particular, at ultralow energies the *R*-matrix theory becomes equivalent to the effective-range theory [32,34] that was used to describe the nonadiabatic attachment process.

It is important to emphasize the difference between the nonpolar target SF_6 and the polar target CH_3I. In the former at ultralow energies nonadiabatic capture into the weakly bound state is nondissociative. In the latter the diffuse dipole-supported state has a short lifetime with respect to predissociation into the valence state of CH_3I^-.

The analysis of available experimental data for free-electron and Rydberg electron attachment to C_{60} suggests that at very low energies *s*-wave capture, possibly mediated by a virtual state, is important, and that a *p*-wave process is dominant above about 3 meV. The p-wave capture model, in contrast to what has been claimed in Refs. [36,37], cannot explain the observed strong temperature dependence of the attachment rate. This dependence is also not compatible with the near-threshold findings of the beam experiments. Further experimental studies, also addressing variation of the rovibrational temperature of C_{60}, are needed to clarify the situation.

ACKNOWLEDGMENTS

This work has been supported by the U.S. National Science Foundation through Grant No. PHY-9801871 and the Deutsche Forschungsgemeinschaft through Forschergruppe Niederenergetische Elektronenstreuprozesse. The authors are grateful to P. D. Burrow, J. Pommier, and M.-W. Ruf for stimulating discussions and for providing data in numerical form. I.I.F. thanks the members of the Forschergruppe for their hospitality during his stay at Fachbereich Physik of the University of Kaiserslautern where this work was initiated and partly accomplished.

[1] H. A. Bethe, Phys. Rev. **47**, 747 (1935); E. P. Wigner, *ibid.* **73**, 1002 (1948).
[2] T. F. O'Malley, Phys. Rev. **150**, 14 (1966).
[3] J. N. Bardsley, J. Phys. B **1**, 349 (1968).
[4] E. Vogt and G. H. Wannier, Phys. Rev. **95**, 1190 (1954).
[5] C. E. Klots, Chem. Phys. Lett. **38**, 61 (1976).
[6] D. Klar, M.-W. Ruf, and H. Hotop, Chem. Phys. Lett. **189**, 448 (1992); D. Klar, M.-W. Ruf, and H. Hotop, Aust. J. Phys. **45**, 263 (1992).
[7] H. Hotop, D. Klar, J. Kreil, M.-W. Ruf, A. Schramm, and J.

M. Weber, in *The Physics of Electronic and Atomic Collisions*, edited by L. J. Dube, J. B. A. Mitchell, J. W. McConkey, and C. E. Brion (AIP Press, Woodbury, NY, 1995), p. 267; A. Schramm, J. M. Weber, J. Kreil, D. Klar, M.-W. Ruf, and H. Hotop, Phys. Rev. Lett. **81**, 778 (1998).

[8] I. I. Fabrikant, Zh. Éksp. Teor. Fiz. **73**, 1317 (1977) [Sov. Phys. JETP **46**, 693 (1977)].

[9] M. T. Frey, S. B. Hill, K. A. Smith, F. B. Dunning, and I. I. Fabrikant, Phys. Rev. Lett. **75**, 810 (1995).

[10] S. B. Hill, M. T. Frey, F. B. Dunning, and I. I. Fabrikant, Phys. Rev. A **53**, 3348 (1996).

[11] L. D. Landau and E. M. Lifshitz, *Quantum Mechanics, Non-Relativistic Theory* (Pergamon, Oxford, 1965).

[12] M. H. Mittleman and R. E. von Holdt, Phys. Rev. **140**, A726 (1965).

[13] I. I. Fabrikant, J. Phys. B **12**, 3599 (1979).

[14] I. I. Fabrikant, Comments At. Mol. Phys. **24**, 37 (1990).

[15] A. Schramm, I. I. Fabrikant, J. M. Weber, E. Leber, M.-W. Ruf, and H. Hotop, J. Phys. B **32**, 2153 (1999).

[16] I. I. Fabrikant, J. Phys. B **11**, 3621 (1978).

[17] A. Herzenberg and B. C. Saha, J. Phys. B **16**, 591 (1983); I. I. Fabrikant, *ibid.* **18**, 1873 (1985).

[18] G. Herzberg, *Infrared and Raman Spectra of Polyatomic Molecules* (D. Van Nostrand, New York, 1945).

[19] P. A. Schulz, R. D. Mead, P. L. Jones, and W. C. Lineberger, J. Chem. Phys. **77**, 1153 (1982); J. R. Smith, J. B. Kim, and W. C. Lineberger, Phys. Rev. A **55**, 2036 (1997).

[20] I. I. Fabrikant and R. S. Wilde, J. Phys. B **32**, 235 (1999).

[21] J. M. Weber, I. I. Fabrikant, E. Leber, M.-W. Ruf, and H. Hotop, Eur. Phys. J. D **11**, 247 (2000).

[22] A. Chutjian and S. H. Alajajian, Phys. Rev. A **31**, 2885 (1985).

[23] A. Schramm, J. M. Weber, J. Kreil, D. Klar, M.-W. Ruf, and H. Hotop, Phys. Rev. Lett. **81**, 778 (1998).

[24] D. Klar, M.-W. Ruf, and H. Hotop, Int. J. Mass Spectrom. (to be published).

[25] D. Klar, M.-W. Ruf, and H. Hotop, Meas. Sci. Technol. **5**, 1248 (1994).

[26] D. Klar, B. Mirbach, H. J. Korsch, M.-W. Ruf, and H. Hotop, Z. Phys. D: At., Mol. Clusters **31**, 235 (1994).

[27] Z. Lj. Petrovic and R. W. Crompton, J. Phys. B **18**, 2777 (1985).

[28] O. J. Orient, A. Chutjian, R. W. Crompton, and B. Cheung, Phys. Rev. A **39**, 4494 (1989).

[29] T. M. Miller, in *CRC Handbook of Chemistry and Physics*, 76th ed., edited by D. R. Lide (CRC Press, Boca Raton, FL, 1995), pp. 10, 192–206.

[30] X. Ling, B. G. Lindsay, K. A. Smith, and F. B. Dunning, Phys. Rev. A **45**, 242 (1992).

[31] F. B. Dunning, J. Phys. B **28**, 1645 (1995).

[32] J. P. Gauyacq and A. Herzenberg, J. Phys. B **17**, 1155 (1984).

[33] O. H. Crawford and B. J. D. Koch, J. Chem. Phys. **60**, 4512 (1974).

[34] J. P. Gauyacq, J. Phys. B **15**, 2721 (1982).

[35] P. D. Burrow, A. Modelli, N. S. Chiu, and K. D. Jordan, J. Chem. Phys. **77**, 2699 (1982).

[36] D. Smith, P. Španel, and T. D. Märk, Chem. Phys. Lett. **213**, 202 (1993).

[37] D. Smith and P. Spanel, J. Phys. B **29**, 5199 (1996).

[38] E. Tosatti and N. Manini, Chem. Phys. Lett. **223**, 61 (1994).

[39] J. Huang, H. S. Carman, Jr., and R. N. Compton, J. Phys. Chem. **99**, 1719 (1995).

[40] Š. Matejčik, T. D. Märk, P. Španel, D. Smith, T. Jaffke, and E. Illenberger, J. Chem. Phys. **102**, 2516 (1995).

[41] T. Jaffke, E. Illenberger, M. Lezius, S. Matejcik, D. Smith, and T. D. Märk, Chem. Phys. Lett. **226**, 213 (1994).

[42] J. M. Weber, M.-W. Ruf, and H. Hotop, Z. Phys. D: At., Mol. Clusters **37**, 351 (1996).

[43] C. D. Finch, R. A. Popple, P. Nordlander, and F. B. Dunning, Chem. Phys. Lett. **244**, 345 (1995).

[44] O. Elhamidi, J. Pommier, and R. Abouaf, J. Phys. B **30**, 4633 (1997).

[45] R. R. Lucchese, F. A. Gianturco, and N. Sanna, Chem. Phys. Lett. **305**, 413 (1999).

[46] F. A. Gianturco, R. R. Lucchese, and N. Sanna, J. Phys. B **32**, 2181 (1999).

[47] E. Fermi, Nuovo Cimento **11**, 157 (1934); For a more detailed discussion of the quasi-free-electron model, see the articles by M. Matsuzawa and by A. P. Hickman, R. E. Olson and J. Pascale, in *Rydberg States of Atoms and Molecules*, edited by R. F. Stebbings and F. B. Dunning (Cambridge University Press, New York, 1983).

[48] C. Desfrançois, H. Abdoul-Carime, and J.-P. Schermann, Int. J. Mod. Phys. B **10**, 1339 (1996).

[49] V. Kasperovich, G. Tikhonov, K. Wong, P. Brockhaus, and V. V. Kresin, Phys. Rev. A **60**, 3071 (1999).

[50] L. D. Landau and E. M. Lifshitz, *Mechanics*, 3rd ed. (Pergamon, Oxford, 1976), Sec. 18.